Journal of Ceramic Processing Research. Vol. 5, No. 3, pp. 232~237 (2004)

J O U R N A L O F
Ceramic Processing Research

Microstructural characteristics and film properties of diamond-like carbon coatings grown by PECVD

Won Jae Yang[a,*], Koichi Niihara[b] and Keun Ho Auh[a]
[a]*Ceramic Processing Research Center (CPRC), Hanyang University, Seoul 133-791, Korea*
[b]*The Institute of Scientific and Industrial Research (ISIR), Osaka University, Ibaraki, Osaka 567-0047, Japan*

Diamond-like carbon (DLC) films were deposited by plasma decomposition of CH_4/H_2 gas mixtures in a RF glow discharge reactor. The chemical structure of diamond-like carbon films deposited at different bias voltages and CH_4 flow contents was investigated by Fourier Transform Infrared (FT-IR) and Raman spectroscopy. An indirect evaluation on the sp^3-bonded carbon in the DLC films was made based on the structural information on the sp^2-bonded carbon obtained from Raman measurements. The mechanical properties of DLC films deposited at different CH_4 flow contents are discussed in terms of Raman parameters such as the position, width and integrated intensities of Raman D and G peaks. The friction coefficient of DLC films was obtained and their frictional behavior was investigated.

Key words: Diamond-like carbon, Raman, Chemical structure, Mechanical property, Friction coefficient.

Introduction

Diamond-like carbon (DLC), called hydrogenated amorphous carbon, films have been a special issue among carbon-based materials because they have interesting properties such as high hardness, high elasticity, low wear and low friction in contact with several materials, high corrosion resistance and optical transparency in the IR region [1-4]. Therefore, they have a potential for use as wear and protective coating layers for magnetic and optical devices [5, 6]. Even though the DLC films have poorer physical properties than diamond films, they exhibit interesting features; (1) deposition at room temperature, (2) superior surface roughness and (3) easy process control for various physical properties. These interesting properties of DLC films arise from their unique microstructure consisting of mixtures of sp^3-bonded and sp^2-bonded carbon. The sp^3-bonded carbon can be a highly cross-linked network appearing as a hard phase, whereas sp^2-bonded carbon gives an open network and appears as a soft phase. The films can be hydrogenated or hydrogen-free depending on the deposition method/conditions and source materials used. Hydrogen incorporated in the films can play a significant role in the bonding configuration, which in some case can stabilize the sp^3-bonded carbon and also affect the microstructure controlling film properties.

The DLC films can be deposited by a variety of methods such as ion beam deposition [7], sputtering [8], plasma enhanced chemical vapor deposition [9], pulsed laser deposition [10] and vacuum arc deposition [11]. These methods are commonly under the control of ion energy which governs the exposure of the substrate and growing film to the precursor ions during the ion bombardment. The ions play an important role in determining the film structures and properties. In the range of low ion energy, the impacting energy of precursor ions into the growing surface is low. The films grown in this range are called ‘polymer-like films’ showing soft and porous characteristics. In the range of medium ion energy, the moderate ion bombardment promotes sp^3 bonding. The films grown in this range are called ‘diamond-like films’ showing hard and dense characteristics. In the range of high ion energy, the fraction of sp^2 bonding in the films increases, resulting in a graphitic phase.

Raman spectroscopy is a useful and effective tool for understanding the chemical structure of amorphous carbon films. Raman measurements are efficient for obtaining information on the chemical structure of molecules in the translation mode with symmetrical bonding configurations. Raman spectra of amorphous carbon films are found to have a significant dependence on the presence of disordered graphite structure [12]. Raman spectra of amorphous carbon are usually fitted with two Gaussian peaks, called the D and G peaks. The parameters (position, width and integrated intensity) of Raman D and G peaks from amorphous carbon films are found to be a probe for their deposition conditions as well as the physical properties of amorphous carbon films. The most remarkable trend of Raman analyses in amorphous carbon films is that the line width narrows

*Corresponding author:
Tel : +82-2-2290-0543
Fax: +82-2-2299-2884
E-mail: wjyang@ihanyang.ac.kr

and D line intensity increases with increasing fraction of sp^2-bonded carbon in the films [13].

As previously mentioned, the key parameter for the growth of DLC films is found to be the precursor ion energy which controls the film structure and properties. The ion energy is proportional to the bias voltage applied to the electrode on which substrates are placed and is in inverse proportion to the reactor pressure. A self-bias voltage can be developed at the powered electrode of the PECVD configuration applied in this study because of the asymmetry between upper and lower electrodes and the difference in the electron and ion mobilities. In this article, we will briefly describe the chemical structure of DLC films deposited by plasma decomposition of CH_4/H_2 gas mixtures with different bias voltages and gas flow contents. Raman understanding will be significantly discussed in terms of Raman parameters obtained from the deposited DLC films. Also, the effects of gas flow contents on the chemical structure and physical properties of DLC films will be investigated.

Experimental procedures

Film deposition

The PECVD system used in this study consisted of a capacitively coupled, asymmetric plasma reactor driven by a 13.56 MHz RF power supply which was connected to the lower electrode. A self-biased negative voltage was developed at the powered electrode due to the asymmetry between the upper and lower electrodes, and the difference in the electron and ion mobilities. The reactor was evacuated by a combination of a mechanical rotary pump and a turbo-molecular pump. The source gases were uniformly distributed by a showerhead type distributor.

The DLC films were grown on Si (100) substrates by plasma decomposition of CH_4/H_2 gas mixtures. Before being loaded in the CVD reactor, Si substrates were ultrasonically cleaned in acetone and ethanol, sequentially. They were then rinsed in de-ionized water. The substrates were loaded in the CVD reactor and then the reactor was evacuated to a base pressure lower than 6.6×10^{-4} Pa. Before the deposition, the surface of the Si substrates was exposed to H_2 plasma operated at a power of 80 W for 10 minutes for *in-situ* cleaning. The surface of Si substrates was exposed to the plasma of CH_4/H_2 gas mixtures for film growth. During the deposition, a self-biased negative voltage was developed at the lower electrode on which the substrates were placed. The bias voltage resulted in ion bombardment to the growing film surface with plasma-decomposed radicals. There was no additional substrate heating during the deposition. When RF power was supplied to the lower electrode, the substrate temperature increased spontaneously. However, the temperature did not exceed 150°C. The CH_4 flow content in the total gas mixture, described as the flow rate of CH_4 gas/(flow rate of CH_4 gas + flow rate of H_2 gas), was varied from 9 to 50%. The bias voltage ranged from 200 to 500 V depending on the applied RF power. The working pressure was kept between 13 and 18 Pa depending on the precursor flow rate.

Film characterization

The chemical structures of grown films were investigated by Fourier Transform Infrared (FT-IR) and Raman spectroscopy. FT-IR spectra were measured in the wavenumber range from 4000-400 cm^{-1}. Raman spectra were obtained in a backscattering geometry using an Ar ion laser excited by a 514.5 nm illumination. Raman spectra ranging from 1000 to 1800 cm^{-1} were fitted by so-called D and G peaks using a Gaussian-curve function. The position, width and relative intensities of each peak were obtained as Raman parameters to examine the chemical structure of the films. The film thickness was monitored by a cross-sectional view in a Scanning Electron Microscope (SEM).

The hardness and modulus ($E/(1-\nu^2)$, E; elastic modulus, ν; Poisson's ratio) of grown films were calculated from the indentation load-depth hysteresis loop obtained by depth-sensing indentation measurements. The elastic modulus itself cannot be determined if the Poisson's ratio is not independently measured [14]. Therefore, in this study, the modulus ($E/(1-\nu^2)$) obtained for a specimen was considered as a measure of the elastic modulus of the film. A Berkovich-type diamond indenter was used to penetrate the sample surface. The indentation tests were performed under an applied load of 2 mN. Indentations were made at 10 different positions on the samples and then averaged.

The friction coefficient of grown films was obtained using a high frequency friction machine with a ball-on-flat configuration. A Co-bonded WC ball (H=15 GPa, 94% WC/6% Co) with a diameter of 12.7 mm was used as a counter material and was moved with a reciprocating sliding geometry at a speed of 54.4 $mm\cdot s^{-1}$ over a non-lubricated film surface with a 5 N load perpendicularly applied to the ball. All the tests were conducted in ambient air at room temperature, where the relative humidity was 30-50%. The friction coefficient of the films was continuously recorded and the values obtained during 80 m sliding were averaged.

Results and Discussion

The chemical structure of grown films was investigated to understand the IR bond characteristics. Figure 1 shows the FT-IR spectra of DLC films deposited at different bias voltages. The characteristic FT-IR spectra of DLC films are shown in a stretching mode in the 3100-2800 cm^{-1} range and a bending mode in the 1700-1300 cm^{-1} range. The C-H stretching appearing at around the 3000 cm^{-1} region was typical of FT-IR

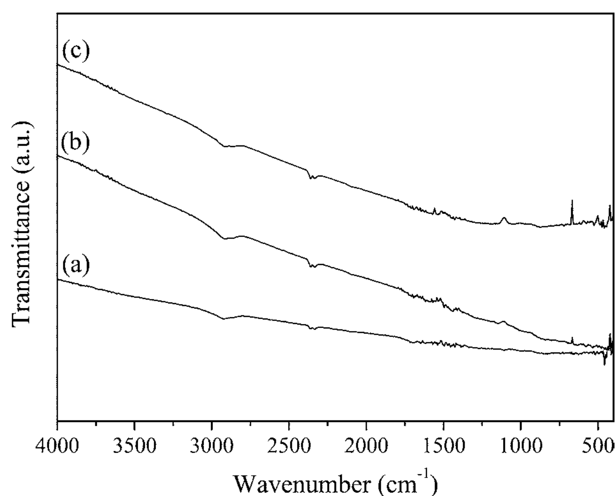

Fig. 1. FT-IR spectra of DLC films deposited at different bias voltages; (a) 200V, (b) 300V and (c) 400V.

bands in the present films. The bands did not show a great difference in their shapes with respect to bias voltages. The spectra in the bending region were not clearly observed because of the background noise, corresponding to the Si substrate. The C-H absorption band in the 3100-2800 cm^{-1} range is typical for sp^3 and sp^2 bonded carbon. This band includes the symmetrical CH_3 stretching at 2870 cm^{-1}, asymmetrical CH_2 stretching at 2920 cm^{-1} and asymmetrical CH_3 stretching at 2965 cm^{-1} corresponding to sp^3 C-H bonds. Also, there are the olefinic C-H stretching bands at 3000 cm^{-1} and 3025 cm^{-1} and aromatic C-H stretching bands at 3050 cm^{-1} corresponding to sp^2 C-H bonds. The FT-IR results revealed that the films were partially hydrogenated consisting of various sp^3- and sp^2-related C-H bonds.

The Raman signal is active in a translation mode with a symmetrical bonding configuration. In single crystalline graphite with a long-range translation symmetry, a sharp peak appears at 1580 cm^{-1} from Raman measurements because the bonding configuration of single crystalline graphite is perfectly symmetrical. The origin of this peak is E_{2g} C-C stretching of the graphite layer, indicating a zone-center mode for graphite crystallites. This peak is called a G peak. Here, G means graphitic. However, an additional translation symmetry mode exists in polycrystalline graphite or amorphous carbon, in which a long-range translation symmetry disappears because of disordering of the ordered graphite structure [15, 16]. This additional translation mode (A_{1g} mode) indicates a zone-edge mode for graphite microcrystallites. This allows an additional peak at 1350 cm^{-1}, called a D peak. Here, D means disordered. Therefore, polycrystalline graphite or amorphous carbon show the feature of both D and G peaks from Raman measurements. Raman parameters such as the position, width and relative intensities of D and G peaks are regarded as graphitization indices of amorphous carbon films. The increase of D peak intensity, the upward shift of the G peak and the narrowing of the G peak width reflect an increase of the sp^2-bonded configuration in amorphous carbon films. These features are explained by an increase of graphite crystallites both in number and size, corresponding to the more pronounced formation of sp^2-bonded carbon and the growth of graphite crystallites, respectively. If the number of graphite crystallites increases, which corresponds to a more disordered graphite structure, the Raman mode corresponding to the A_{1g} translation becomes more active. Therefore, the intensity of the D peak increases, resulting in an increase of the relative integrated intensities of D and G peaks (I_D/I_G ratio). The increase of graphite crystallites in size indicates a growth of sp^2-bonded clusters. Therefore, a full symmetry of the E_{2g} translation mode becomes more active, resulting in an upward shift of the G peak and a narrowing of the G peak width due to an increased ordering of the graphite structure. The structure in DLC films is found to be a mixture of sp^3-bonded and sp^2-bonded carbon, suggesting a structural model with the sp^2-bonded carbon clusters embedded in a sp^3-bonded carbon matrix which may be partially hydrogenated [17]. The visible Raman spectrum, applied in this study, is more sensitive to sp^2-bonded carbon [13, 18]. Therefore, an indirect evaluation of the sp^3-bonded carbon could be made based on the structural information from the sp^2-bonded carbon obtained from Raman measurement.

Figure 2 shows Raman parameters obtained from Gaussian curve-fitting in Raman spectra of DLC films deposited at different bias voltages and CH_4 flow contents. The I_D/I_G ratio increased with an increase of bias voltage and decrease of CH_4 flow content. Also, the G peak position shifted to a higher wavenumber with an increase of bias voltage and decrease of CH_4 flow content. The variation of the G peak width showed a narrowing tendency with an increase of bias voltage and decrease of CH_4 flow content. An increase of I_D/I_G ratio, G peak narrowing and upward shift of the G peak indicates an increase of sp^2-bonded carbon in the films. Therefore, the fraction of sp^2-bonded carbon in the film increased with an increase of bias voltage and decrease of CH_4 flow content. The excessive ion energy from the higher bias voltage resulted in an annealing of the graphite-like structure with a higher fraction of sp^2-bonded carbon. At low bias voltage in the range examined, the CH_4 flow content did not affect significantly the structural formation of DLC films, which describes the relative amounts of sp^3-bonded and sp^2-bonded carbon in the films. However, the effect of CH_4 flow content on the structural formation of DLC films became pronounced with an increase of bias voltage. An increase of bias voltage made a larger structural modification of DLC films at low CH_4 flow content. Below the medium bias voltage, the higher concentrations of hydrocarbon radicals were

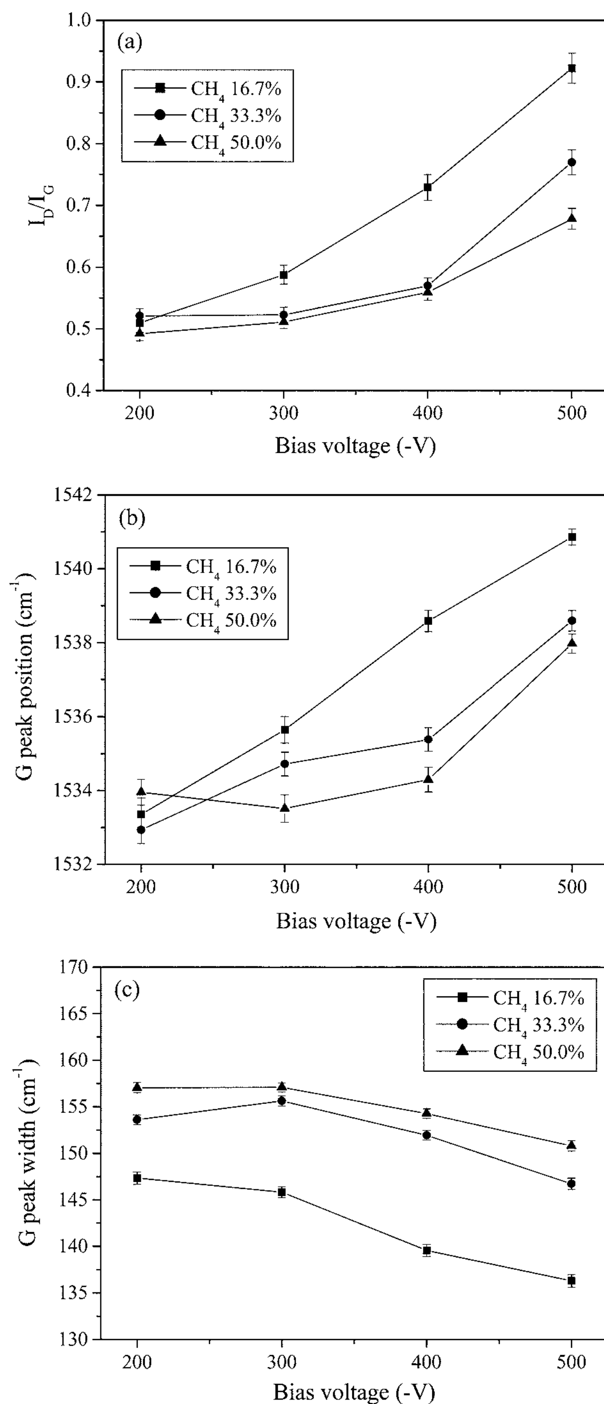

Fig. 2. Raman parameters obtained from Gaussian curve-fitting in Raman spectra of DLC films deposited at different bias voltages and CH_4 flow contents; (a) I_D/I_G ratio, (b) G peak position and (c) G peak width.

effective in preventing structural transitions of DLC films to a graphite-like structure, which is usual at high bias voltage. As the fraction of hydrocarbon radicals increased, the sp^3-bonded carbon component increased, indicating an enhanced cross-linking of sp^3-bonded carbon during the film growth. However, even higher concentrations of hydrocarbon radicals could not prevent the structural transitions of DLC films to a graphite-like structure at high bias voltage.

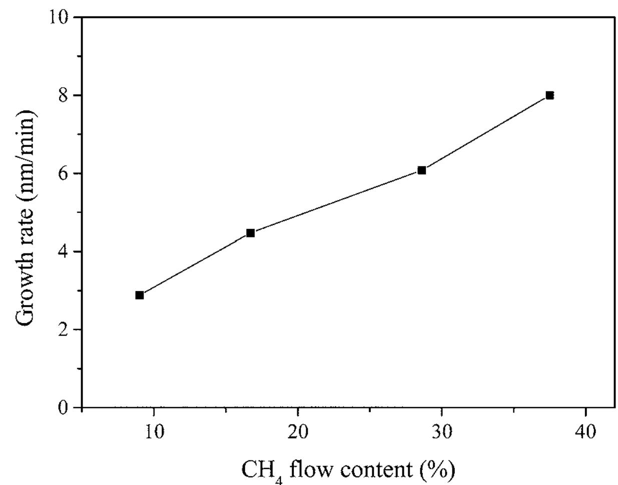

Fig. 3. Growth rate of DLC films as a function of CH_4 flow content.

Figure 3 shows the growth rate of DLC films deposited at different CH_4 flow contents. As the CH_4 flow content increased, the growth rate of DLC films increased, as expected. When the flow rate of CH_4 gas increased, the working pressure also increased because CH_4 gas is heavier than H_2 gas. If the pressure increases, the mean free path of chemical species becomes shorter. There-

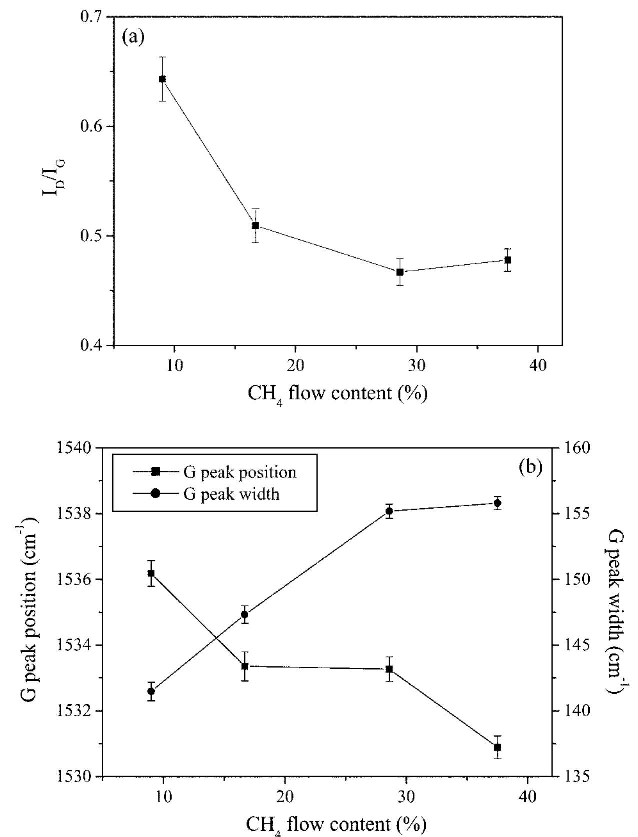

Fig. 4. Raman parameters obtained from Gaussian curve-fitting in Raman spectra of DLC films deposited at different CH_4 flow contents; (a) I_D/I_G ratio and (b) G peak position and width.

fore, the ion bombardment to the substrate would be limited due to the collision between each chemical species in the reactor. However, the higher growth rate in the higher CH_4 flow contents means that the effect of the concentration of chemical species on the growth rate was more significant than was the working pressure.

Figure 4 shows the Raman parameters obtained from Gaussian curve fitting in Raman spectra of DLC films deposited at different CH_4 flow contents. As the CH_4 flow content increased, the I_D/I_G ratio decreased. Also, the G peak position was shifted to a lower wavenumber and the G peak width became broader with an increase of the CH_4 flow content. This structural information means that the fraction of sp^3-bonded carbon increased in the film as the CH_4 flow content increased. Figure 5 shows the mechanical properties of DLC films deposited at different CH_4 flow contents. The hardness values ranged from 12.8 to 19.9 GPa and the elastic modulus values ranged from 135.0 to 171.8 GPa depending on the CH_4 flow content. As the CH_4 flow content increased, the hardness and elastic modulus of the films increased. This result implies that the fraction of sp^3-bonded carbon increased with an increase of hydrocarbon radicals in the plasma during the film growth, as expected from the structural information of Raman parameters. The results show that with an increase of the concentration of hydrocarbon radicals, the formation and growth of graphite crystallites or the transition of sp^3-bonded carbon to sp^2-bonded carbon would be suppressed and then the cross-linking of sp^3-bonded carbon would be promoted. The elastic modulus of a material represents the relative stiffness of the material within the elastic range, which indicates the resistance not to be separated with neighboring atoms. The elastic modulus is dependent on the binding energy between the atoms. A film with a high value of elastic modulus thus implies that the film consists

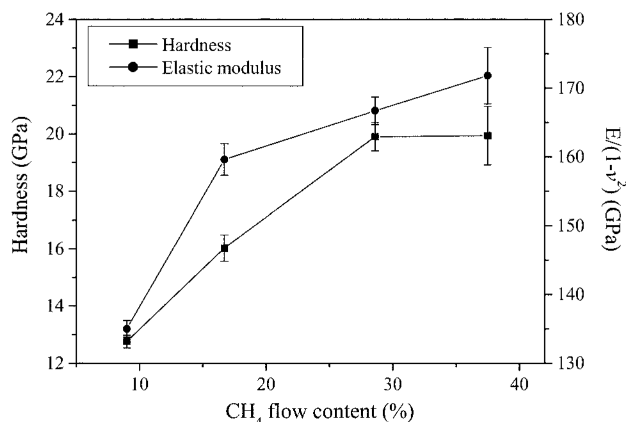

Fig. 5. Hardness and elastic modulus of DLC films deposited at different CH_4 flow contents.

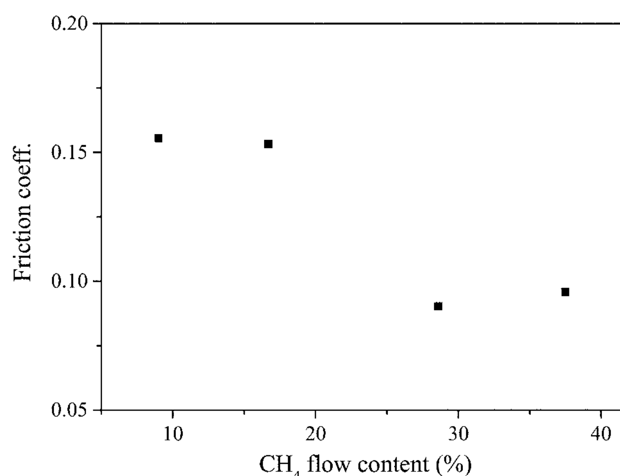

Fig. 6. Friction coefficient of DLC films as a function of CH_4 flow content.

largely of rigid network structures with strong C-C bonding and with a lower contribution of weak C-H bonding. Therefore, the fraction of C-C bonding in the films was found to increase with an increase of CH_4 flow content.

The wear characteristics of DLC films were investigated by measuring the friction coefficient. Figure 6 shows the friction coefficient of DLC films as a function of CH_4 flow content. With an increase of CH_4 flow content, the friction coefficient decreased from 0.15 to 0.1. The frictional behavior of the DLC films made here can be explained in terms of hardness values. As previously stated, the hardness of DLC films increased with an increase of CH_4 flow content. It was reported that the low friction coefficient of DLC films can be achieved by the formation of a friction-induced graphite layer on the top surface of a DLC film [19, 20]. The frictional force is ideally the product of shear strength and contact area [21]. The interfacial shear strength will be reduced because the shear will take place within the transferred soft graphite layer. Also, the hard underlying DLC film can support the load, which will reduce the contact area. The friction coefficient is equal to the frictional force divided by the applied load. The films with a higher hardness can provide a reduced frictional force and consequently a reduced friction coefficient. Therefore, the lower friction coefficient of the films deposited at higher CH_4 flow content can be explained by their higher hardness, which can support the load efficiently and thus reduce the contact area. The lower film thickness in accordance with a lower growth rate at lower CH_4 flow content may be one of the reasons that the friction coefficient is relatively high at lower CH_4 flow content because the film with a low thickness could not support the load so well.

Conclusions

The structural information on DLC films was obtained by FT-IR and Raman measurements. The DLC films made here were partially hydrogenated and consisted of various sp^3- and sp^2-related C-H bonds. The chemical structure of DLC films was investigated under different bias voltages and gas flow contents by comparing Raman parameters such as the position, width and relative intensities of D and G peaks, which are regarded as graphitization indices of amorphous carbon films. The lower bias voltage in the range examined and the higher CH_4 flow content allowed a higher fraction of sp^3-bonded carbon in the films, resulting in the promotion of mechanical properties. Below a medium bias voltage, the higher CH_4 flow contents were effective in preventing the transitions of DLC films to a graphite-like structure, which is usual at high bias voltage. The hardness and elastic modulus of DLC films increased with an increase of CH_4 flow content, which are with the structural information obtained from Raman measurements. Furthermore, the films deposited at higher CH_4 flow contents showed lower friction coefficients, which results from their higher hardness, resulting in a reduction of contact area by efficient load support during the friction test.

Acknowledgements

This study was financially supported by the Korean Science and Engineering Foundation (KOSEF) through the Ceramic Processing Research Center (CPRC) and also by the Core University Program between Hanyang University, Korea and Osaka University, Japan.

References

1. E.I. Meletis, A. Erdemir, and G.R. Fenske, Surf. Coat. Technol. 73 (1995) 39-45.
2. Z. Sun, C.H. Lin, Y.L. Lee, J.R. Shi, B.K. Tay, and X. Shi, Thin Solid Films 377-378 (2000) 198-202.
3. P.P. Psyllaki, M. Jeandin, D.I. Pantelis, and M. Allouard, Surf. Coat. Technol. 130 (2000) 297-303.
4. A. Erdemir, O.L. Eryilmaz, I.B. Nilufer, and G.R. Fenske, Diamond Relat. Mater. 9 (2000) 632-637.
5. J. Esteve, M.C. Polo, and G. Sanchez, Vacuum 52 (1999) 133-139.
6. A.B. Vladimirov, I.Sh. Trakhtenberg, A.P. Rubshtein, S.A. Plotnikov, O.M. Bakunin, L.G. Korshunov, and E.V. Kuzmina, Diamond Relat. Mater. 9 (2000) 838-842.
7. R.W. Lamberton, J.F. Zhao, D. Magill, J.A. McLaughlin, and P.D. Maguire, Diamond Relat. Mater. 7 (1998) 1054-1058.
8. K. Bewilogua, C.V. Cooper, C. Specht, J. Schröder, R. Wittorf, and M. Grischke, Surf. Coat. Technol. 127 (2000) 224-232.
9. K.J. Clay, S.P. Speakman, N.A. Morrison, N. Tomozeiu, W.I. Milne, and A. Kapoor, Diamond Relat. Mater. 7 (1998) 1100-1107.
10. K. Miyoshi, B. Pohlchuck, K.W. Street, J.S. Zabinski, J.H. Sanders, A.A. Voevodin, and R.L.C. Wu, Wear 225-229 (1999) 65-73.
11. I.I. Aksenov, V.A. Belous, V.V. Vasilíev, Yu. Ya. Volkov, and V.E. Strelínitskij, Diamond Relat. Mater. 8 (1999) 468-471.
12. R.O. Dillon and J.A. Woollam, Phys. Rev. B 29[6] (1984) 3482-3489.
13. M.A. Tamor and W.C. Vassell, J. Appl. Phys. 76[6] (1994) 3823-3830.
14. W.J. Meng, T.J. Curtis, L.E. Rehn, and P.M. Baldo, J. Appl. Phys. 83[11] (1998) 6076-6081.
15. D. Beeman, J. Silverman, R. Lynds, and M.R. Anderson, Phys. Rev. B 30[2] (1984) 870-875.
16. F. Tuinstra and J.L. Koenig, J. Chem. Phys. 53[3] (1970) 1126-1130.
17. J. Robertson and E.P. O'Reilly, Phys. Rev. B 35[6] (1987) 2946-2957.
18. D. Sheeja, B.K. Tay, K.W. Leong, and C.H. Lee, Diamond Relat. Mater. 11 (2002) 1643-1647.
19. Y. Liu, A. Erdemir, and E.I. Meletis, Surf. Coat. Technol. 94-95 (1997) 463-468.
20. Y. Liu and E.I. Meletis, J. Mater. Sci. 32 (1997) 3491-3495.
21. K. Holmberg and A. Matthews, in: D. Dowson (Ed.), Coatings Tribology-Properties, Techniques and Applications in Surface Engineering, Elsevier, Amsterdam, 1994, p. 93.